

## Anomalous Strain Relaxation in SiGe Thin Films and Superlattices

F. K. LeGoues, B. S. Meyerson, and J. F. Morar

*IBM Research Division, T. J. Watson Research Center, Yorktown Heights, New York 10598*

(Received 18 January 1991)

We describe anomalous strain relaxation in graded SiGe superlattices and thin films. This relaxation is characterized by the presence of dislocations in the Si substrate, as well as in the lower part of the film or superlattice, and results in a dislocation-free top layer. This challenges the basic assumption, dating back to Van der Merwe, that the substrate does not participate in the strain-relief process. We show that this phenomenon is due to the paucity of nucleation sites, and controlled by the specific Ge concentration profile in the film. Relaxed, defect-free  $\text{Si}_x\text{Ge}_{1-x}$  films containing up to 60% Ge have been grown in this manner.

PACS numbers: 68.55.Ln

Strain and strain relief play a crucial role in determining the properties of thin films and superlattices. Indeed, the ability to influence the formation and propagation of dislocations in strained materials can dramatically expand opportunities for combining materials such as Si and Ge which have a 4% lattice mismatch. However, to fully access the promise of the SiGe system, it is necessary to grow thick, relaxed, SiGe alloys on Si substrates.<sup>1</sup> This is a very challenging problem, because the relaxation mechanism involves the motion of threading dislocations through the thin film. These threading defects can become pinned, e.g., by intersecting dislocations,<sup>2,3</sup> resulting in a relaxed, but extremely defective thin film.

In this paper, we describe, and propose a model for, a novel growth mechanism which solves this major technological challenge: Control of threading dislocations has been achieved, such that relaxed layers of arbitrary composition have been grown defect free to a level previously unattainable. The strain-relieving defects are buried in a compositionally graded buffer layer as well as deep into the substrate itself, which challenges the basic assumption, dating back to Van der Merwe<sup>4</sup> and Matthews and Blakeslee,<sup>5</sup> that the substrate will not participate in the strain-relief process.

Figure 1 illustrates the problem: In Fig. 1(a), a 5000-Å layer of constant composition,  $\text{Si}_{75}\text{Ge}_{25}$ , has been grown by UHV chemical-vapor deposition (CVD) on Si(100). The SiGe is relaxed, but a typical, dense network of threading dislocations is clearly seen, rendering any technological application of such a film at the very least difficult. Figure 1(b) shows a "graded layer" (the Ge composition varies linearly from 0% to 25%), where the top layer of the film is also relaxed (see results further in the text). Here, the network of dislocations is confined to the lower part of the film, and, most surprisingly, deep into the substrate itself, leaving the top part of the film defect free. We note that this is similar to recently published results,<sup>6</sup> in which a graded superlattice (the Ge concentration increases from one superlattice layer to the next, instead of varying linearly) displayed the same general behavior. In the present paper, we propose a mechanism for this phenomenon that explains the presence of dislocation deep in the Si substrate, as well

as the absence of threading defects in the top portion of the thin film. We also determine the critical parameters controlling this process.

We note that this behavior is completely different from the well-known technique of filtering, first discussed by Matthews and Blakeslee.<sup>7</sup> Filtering consists of using strained superlattices to bend threading dislocations to the edge of the wafer. It has been used successfully in GaAs-based systems,<sup>8</sup> but has been shown to fail in the SiGe system.<sup>9</sup> Further, even in systems where filtering does work, a reduction in the density of threading dislocations of  $10^4$  has been achieved,<sup>8</sup> while we will show that reductions of more than  $10^7$  are achieved here. Finally, filtering does not result in dislocations being injected into the substrate. Here, we have actually modified the nucleation of dislocations, and increased the mobility of the threading segments, to such an extent that layers containing up to 60% Ge have been grown completely relaxed and dislocation free.

Samples were grown by both UHV-CVD and molecular-beam epitaxy (MBE) at temperatures of about 500°C. Cleaning and growth procedures have been described for both techniques respectively in Refs. 10 and 11. Samples were prepared for both planar-view and

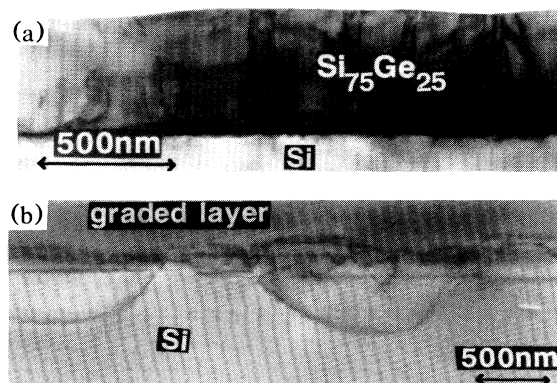


FIG. 1. Cross-sectional images of two samples grown by UHV-CVD, in the same experimental conditions (temperature, pressure, etc.). (a) Uniform layer containing 25% Ge. (b) Graded layer, where the Ge composition varies linearly from 0% to 25% throughout the film.

cross-sectional TEM by mechanically thinning to about  $30\ \mu\text{m}$ , followed by ion milling to electron transparency. The observations were made at 300 kV, except for the convergent-beam patterns, which were obtained at 100 kV.

Figure 2 shows a sample grown by CVD, consisting of a graded superlattice topped with a 4000-Å-thick layer containing 20% Ge. Figure 2(a) shows a cross-sectional view, and demonstrates that the top layer is dislocation free. The dislocations are located in the graded superlattice, as well as in the Si substrate itself. Planar-view TEM was also done on the same sample, in order to quantify the quality of the top layer. We estimate<sup>12</sup> that a reduction of in excess of  $10^7$  has been achieved, leaving the top layer at a dislocation density below  $10^4/\text{cm}^2$ . In order to ascertain the degree of relaxation in the top layer, we did convergent-beam-diffraction studies.<sup>13</sup> This was done by cross sectioning the sample along the (100) direction [instead of the more usual (110) direction], and cooling it in the microscope to about  $-140^\circ\text{C}$  in order to obtain sharp convergent-beam patterns. Figures 2(b) and 2(c) show the center spots of patterns obtained from the Si substrate far away from the interface, and from

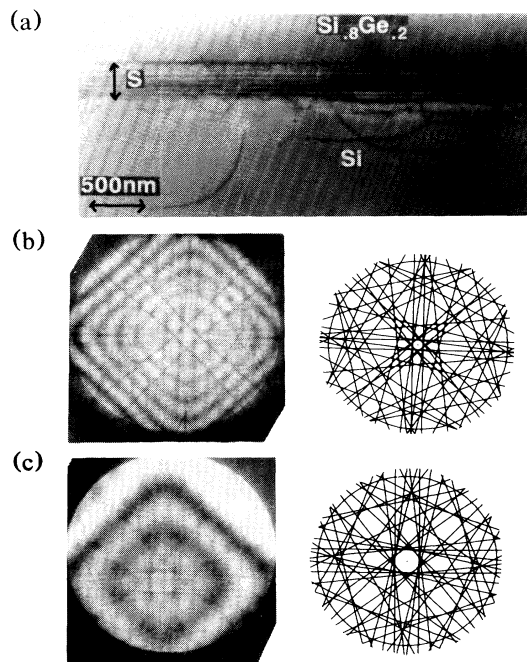


FIG. 2. Graded superlattice, topped with a 4000-Å-thick, uniform layer containing 20% Ge (grown by CVD). (a) Cross-sectional image.  $S$  indicates the position of a graded superlattice, consisting of the following structure: 200 Å  $\text{Si}_{95}\text{Ge}_5$ , 50 Å Si, 200 Å  $\text{Si}_{90}\text{Ge}_{10}$ , 50 Å Si, ( $\text{Si}_{85}\text{Ge}_{15}/50\ \text{Å Si}$ ) 3 times,  $\text{Si}_{82}\text{Ge}_{18}$ , 50 Å Si. (b) Center spot, and corresponding simulation, of the convergent-beam pattern obtained from the Si substrate, far away from the superlattice. Note that the cross section in this case is along (100), while the micrograph was obtained by cross sectioning along (110). (c) Same, from the top layer containing 20% Ge.

the top layer containing 20% Ge. Simulated convergent-beam patterns<sup>14</sup> are also included, demonstrating that, using the Si lattice as a reference, we can determine the lattice parameter of the top layer to correspond to a relaxed  $\text{Si}_{80}\text{Ge}_{20}$  film. The relaxation can actually be deduced simply by noting that, even though the experimental pattern shown in 2(c) is qualitatively very different from that shown in 2(b), the square symmetry has been retained, indicating no tetragonal distortion in the top layer, and thus no strain within the detectability limit of the convergent-beam technique (distortions resulting in changes in the lattice parameter of 0.1% would be detectable by this technique<sup>13</sup>).

Several experiments were performed to ascertain the parameters controlling this novel relaxation mechanism. First, we observe these results to be independent of growth technique: The samples shown in Fig. 2(a) (grown by CVD) and Fig. 3(a) (grown by MBE) exhibit the same type of dislocation network. Second, we observe that these results depend critically on the perfection of the growth interface: The samples in Figs. 3(a) and 3(b) were grown under identical conditions, except for the introduction of a Si buffer layer in 3(a), which buried particulates that appear after extended heating of the sample during cleaning. The only difference between the samples was therefore the perfection of the initial surface upon which alloys were deposited. Third, we observe that a good starting surface is not sufficient to avoid threading dislocations, as illustrated in Fig. 1(a), where a 25% Ge layer is grown on a substrate prepared identically to that in 1(b). Finally, we observe that similar dislocation structures result independently of how the Ge concentration is increased, either continuously [Fig. 1(a)] or in steps [Fig. 3(a)].

In order to characterize the dislocation network,

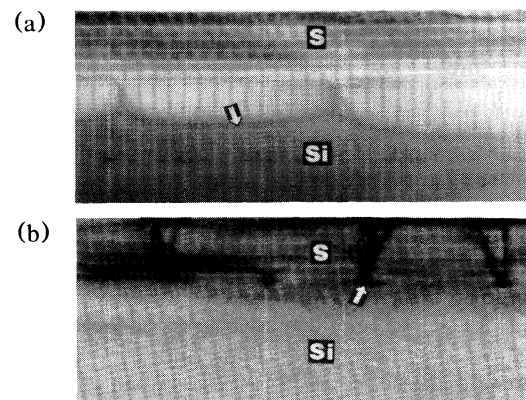


FIG. 3. (a) Sample grown by MBE. The graded superlattice indicated by  $S$  has the same structure as the one shown in Fig. 2. The arrow indicates one dislocation located in the Si substrate. (b) Sample grown identically to (a), but without a buffer Si layer. Particles are clearly seen at the graded superlattice interface. The arrow indicates one particle from which a network of threading dislocations emerges.

cross-sectional TEM samples were viewed perpendicular to the (110) direction (Figs. 1, 2, and 3). By tilting the sample about  $30^\circ$  around the  $[1\bar{1}0]$  direction, dislocations which had previously run parallel to the electron beam became visible as lines, as shown in Fig. 4. These dislocations are located deep within the Si substrate and are part of a "pileup" of dislocations which have glided along a single (111) plane, typical of a nucleation source located at the top of the pileup.<sup>15</sup> We performed  $\mathbf{g} \cdot \mathbf{b}$  analysis to determine the Burgers vector of the dislocations in a pileup. This demonstrates that all the dislocations in one pileup have the same Burgers vector, and are of the  $\frac{1}{2}(10\bar{1})$  type, i.e., glissile on the (111) plane. Note that the dislocations that are seen to "loop" into the Si substrate [Figs. 1(b) and 2(a)] are of the same nature, but imaged in a direction perpendicular to the ones imaged here in the pileup.

We propose a two-step mechanism that explains these experimental observations. First, at a thickness significantly greater than the equilibrium critical thickness, a few dislocations are introduced, possibly as half loops from the surface, or as loops nucleated at defects in the film (such as the diamond-shaped defects described by Eaglesham *et al.*<sup>16</sup>). Second, the network thus formed and, in particular, the nodes formed by intersecting dislocations begin acting as Frank-Read sources,<sup>15</sup> generating additional dislocations, as needed to relieve the increasing strain of the graded layer or superlattice. This mechanism explains the two striking features of the final microstructure, i.e., the presence of dislocations deep inside the substrate, and the lack of threading dislocations in the top layer. Let us examine these phenomena one at a time.

The presence of dislocations deep inside the substrate is a direct consequence of the activation of Frank-Read sources as a mechanism to generate new dislocations to relieve the misfit. Let us consider a segment of an interfacial dislocation pinned at two nodes by intersecting dislocations [Fig. 5(a)]. It will start operating as a Frank-Read source by bowing out into the substrate [Fig. 5(b)]. It will then loop into the thin film, until it

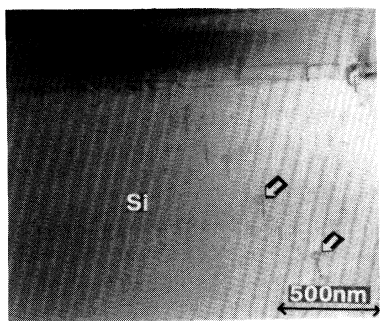


FIG. 4. Graded sample, grown by CVD, cross sectioned perpendicular to the (110) direction, and tilted by  $30^\circ$  around  $[1\bar{1}0]$ , so as to image the dislocations lying along (110). The arrows indicate two dislocations at the bottom of the pileup.

reaches the surface, becoming in effect a half loop [Figs. 5(c) and 5(d)]. The first loop formed in this manner is not expected to penetrate very deep into the substrate, because it is energetically rather costly to introduce dislocations into a substrate that is, for all practical purposes, not strained. Thus, unlike the typical Frank-Read source, this first loop is expected to be very elongated along the interface and into the thin film. Eventually though, as more loops form, each new loop will push the preceding one further down, thus the very deep, typical, pileups observed [Figs. 5(e) and 4]. Careful calculations on the forces exerted on the pinned segment of the dislocation by the compressive stress in the film and the nearby dislocations have to be done in order to explain the unexpected bowing of the initial dislocations into the Si substrate.

This brings us to the second feature of this growth mode, i.e., the lack of threading dislocations in the top part of the thin film: Once a loop has grown large enough so that it has intersected the growth surface, it becomes a half loop, and can start relieving the misfit in a way exactly similar to that described by Matthews and Blakeslee.<sup>5</sup> Each threading part of the half loop moves under the influence of the stress. The motion of these threading dislocations leaves behind a misfit dislocation [Figs. 5(d) and 5(e)]. What is striking here is that at no point do the threading dislocations become pinned, which would result in the typical microstructure shown in Fig. 1(a). One thus has to conclude that each threading segment has moved all the way to the edge of the wafer. In some of the experiments described here, growth was done on 5-in. wafers, so that the dislocations had to move at a rate of about  $10 \mu\text{m}/\text{sec}$ , which at the growth temperature of  $550^\circ\text{C}$  is several orders of magnitude faster than expected from previous measurements.<sup>17</sup>

In contrast, during "normal" growth [see Fig. 1(a), for example] dislocations become pinned, leaving the

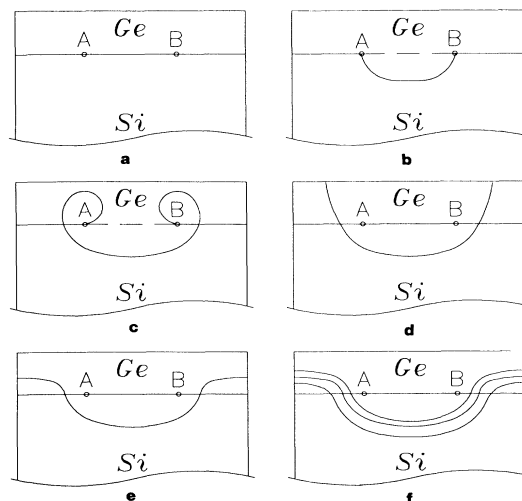


FIG. 5. Schematic representation of the second step of dislocation formation.

thin film defective. Hull, Bean, and Buescher,<sup>2</sup> and later Freund,<sup>3</sup> addressed this question and showed that the repulsive force between a moving threading dislocation and a perpendicular dislocation can be enough to pin the threading part. In order for a threading dislocation to bypass a perpendicular dislocation, a certain "excess stress" needs to be applied, i.e., the film needs to be grown significantly past the equilibrium critical thickness. In the present study, the grading of the interface helps reduce the number of threading defects in two ways. First, the initial nucleation of dislocations is retarded, possibly because it is easier to grow a perfect interface when the difference of composition between film and substrate is small. Thus, when the initial network of dislocations is formed, there is a very high driving force for moving the threading dislocations all the way to the edge of the wafer. As additional dislocations are formed though, and the stress thus decreases, this driving force would also decrease, so that, eventually, the threading parts should become pinned. This is where the grading plays its second, most critical, role: As each new dislocation loop is formed, and as each new thread moves toward the edge of the wafer, the grading provides "fresh" interfaces, with few preexisting dislocations on which a thread could become pinned. If we consider the case of the linearly graded film, each atomic layer in the thin film needs to achieve its own lattice parameter in order to minimize the energy; thus, in principle, one "layer" of dislocations is needed at each atomic plane, which in effect spreads the total dislocation network over the compositionally graded region [Fig. 5(f)]. Consequently, at each layer, there are far fewer dislocations, and thus far fewer chances for a threading segment to become pinned by an intersecting dislocation.

This phenomenon is dependent upon the slope of the grading; i.e., there is probably a "critical slope" above which the dislocation interaction is strong enough to pin down the threads. We are now in the process of investigating this concept. The case of the graded superlattice is similar except that here the "grading" of the dislocation network will occur in a stepwise manner, rather than linearly. Intersecting dislocations are not the only way to pin dislocations. As seen in Fig. 3(b), particulates at the interface can play the same role and, in this particular case, are indeed more efficient at pinning threading segments than intersecting dislocations. Similar defects, or ones such as those described by Eaglesham *et al.*,<sup>16</sup> may also prevent the mechanism from operating, by providing numerous low-energy nucleation sites: It is evident that the Frank-Read-type source described here will only operate in cases when no other nucleation sites are provided. This may explain why this phenomenon has not been observed before.

This work shows a new source of dislocations in thin

films, that operates only in very specific cases where no low-energy nucleation sites are present. Unlike cases described previously, and contrary to theoretical predictions, dislocation formation results in the substrate itself being significantly strained by the introduction of a large number of pileups. As was previously pointed out,<sup>18</sup> this shows that the notion of critical thickness is meaningless unless one takes into account the exact defect being formed and its energy of formation. Finally, this work may have significant impact on technology since it opens up the possibility of growing relaxed, dislocation-free SiGe alloys on Si substrates. We have successfully used this technique to grow such layers containing up to 60% Ge. This technique should work all the way to pure Ge layers.

<sup>1</sup>D. W. Goodman, Y. I. Nissin, and E. Rosencher, in *Heterostructures on Silicon: One Step Further with Silicon* (Kluwer, Dordrecht, Boston, and London, 1989).

<sup>2</sup>R. Hull, J. C. Bean, and C. Buescher, *J. Appl. Phys.* **66**, 5837 (1989).

<sup>3</sup>L. B. Freund, *J. Appl. Phys.* **68**, 2073 (1990).

<sup>4</sup>J. H. van der Merwe, *J. Appl. Phys.* **34**, 117 (1963).

<sup>5</sup>J. W. Matthews and A. E. Blakeslee, *J. Cryst. Growth* **29**, 273 (1975).

<sup>6</sup>B. S. Meyerson, K. J. Uram, and F. K. LeGoues, *Appl. Phys. Lett.* **53**, 2555 (1988).

<sup>7</sup>J. W. Matthews and A. E. Blakeslee, *J. Cryst. Growth* **32**, 265 (1976).

<sup>8</sup>B. W. Dodson, *J. Electron. Mater.* **19**, 503 (1990).

<sup>9</sup>R. Hull, J. C. Bean, R. E. Leibenguth, and D. J. Werder, *J. Appl. Phys.* **65**, 4723 (1989).

<sup>10</sup>B. S. Meyerson, F. Himpfel, and K. J. Uram, *Appl. Phys. Lett.* **57**, 1034 (1990).

<sup>11</sup>The (100) surfaces were prepared similarly to those described in J. F. Morar and M. Wittmer, *Phys. Rev. B* **37**, 2618 (1988).

<sup>12</sup>An estimate of the reduction in dislocation density is obtained as follows. We obtained several low magnification ( $\times 2100$ ) planar-view pictures. No dislocations were found in any picture; thus, a highest possible number for the dislocation density can be obtained by assuming that one single dislocation was present in the surveyed area, which lead to a density of  $10^4/\text{cm}^2$ . From the sample shown on Fig. 1(a) (as well as from the literature), we estimate a threading dislocation density of about  $10^{11}/\text{cm}^2$ . Thus the reduction is at least  $10^7$ .

<sup>13</sup>J. M. Cowley, *Adv. Electron. Electron Phys.* **46**, 1 (1978).

<sup>14</sup>The simulations were done using P. A. Stadelman's program. For details, see *Ultramicroscopy* **21**, 131 (1987).

<sup>15</sup>J. P. Hirthe and J. Lothe, in *Theory of Dislocations* (Wiley, New York, 1982), 2nd ed.

<sup>16</sup>D. J. Eaglesham, E. P. Kvam, D. M. Maher, C. J. Humphreys, and J. C. Bean, *Philos. Mag.* **59**, 1059 (1989).

<sup>17</sup>R. Hull, J. C. Bean, D. J. Werder, and R. E. Leibenguth, *Phys. Rev. B* **40**, 1681 (1989).

<sup>18</sup>F. K. LeGoues, M. Copel, and R. M. Tromp, *Phys. Rev. Lett.* **63**, 1826 (1989).

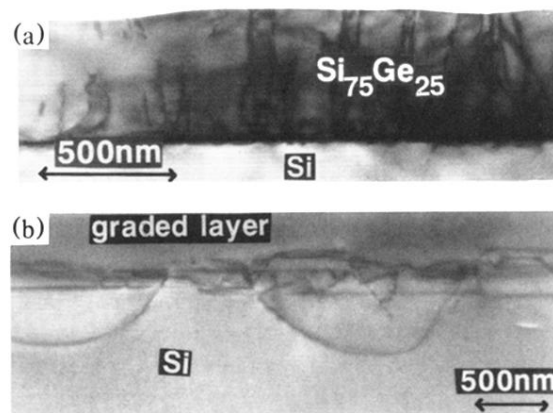


FIG. 1. Cross-sectional images of two samples grown by UHV-CVD, in the same experimental conditions (temperature, pressure, etc.). (a) Uniform layer containing 25% Ge. (b) Graded layer, where the Ge composition varies linearly from 0% to 25% throughout the film.

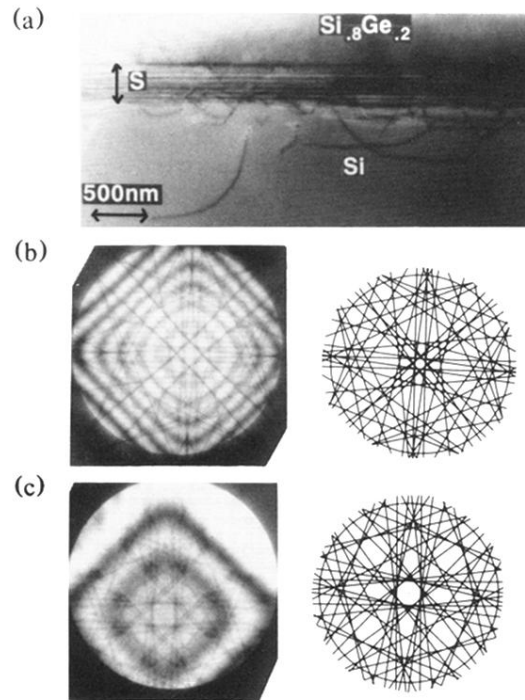


FIG. 2. Graded superlattice, topped with a 4000-Å-thick, uniform layer containing 20% Ge (grown by CVD). (a) Cross-sectional image. *S* indicates the position of a graded superlattice, consisting of the following structure: 200 Å  $\text{Si}_{95}\text{Ge}_5$ , 50 Å Si, 200 Å  $\text{Si}_{90}\text{Ge}_{10}$ , 50 Å Si, ( $\text{Si}_{85}\text{Ge}_{15}/50$  Å Si) 3 times,  $\text{Si}_{82}\text{Ge}_{18}$ , 50 Å Si. (b) Center spot, and corresponding simulation, of the convergent-beam pattern obtained from the Si substrate, far away from the superlattice. Note that the cross section in this case is along (100), while the micrograph was obtained by cross sectioning along (110). (c) Same, from the top layer containing 20% Ge.

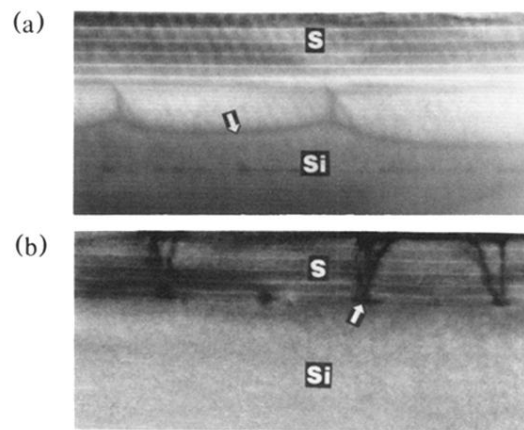


FIG. 3. (a) Sample grown by MBE. The graded superlattice indicated by  $S$  has the same structure as the one shown in Fig. 2. The arrow indicates one dislocation located in the Si substrate. (b) Sample grown identically to (a), but without a buffer Si layer. Particles are clearly seen at the graded superlattice interface. The arrow indicates one particle from which a network of threading dislocations emerges.

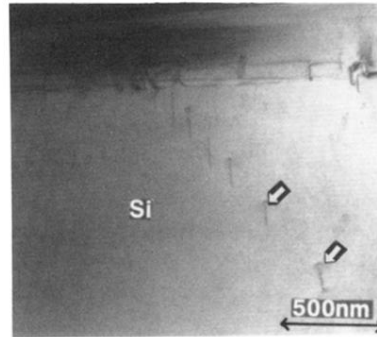


FIG. 4. Graded sample, grown by CVD, cross sectioned perpendicular to the  $(110)$  direction, and tilted by  $30^\circ$  around  $[1\bar{1}0]$ , so as to image the dislocations lying along  $(110)$ . The arrows indicate two dislocations at the bottom of the pileup.